





## Article

# Performance Analysis of a Solar Cooling System with Equal and Unequal Adsorption/Desorption Operating Time

Farkad A. Lattieff <sup>1</sup>, Mohammed A. Atiya <sup>2</sup>, Jasim M. Mahdi <sup>1</sup> , Hasan Sh. Majdi <sup>3</sup> ,  
Pouyan Talebizadehsardari <sup>4,\*</sup>  and Wahiba Yaïci <sup>5,\*</sup> 

<sup>1</sup> Department of Energy Engineering, University of Baghdad, Baghdad 10071, Iraq; farkad500@gmail.com (F.A.L.); jasim@siu.edu (J.M.M.)

<sup>2</sup> Al-Khwarizmi College of Engineering, University of Baghdad, Baghdad 10071, Iraq; mohatiya1965@gmail.com

<sup>3</sup> Department of Chemical Engineering and Petroleum Industries, Al-Mustaqbal University College, Babylon 51001, Iraq; hasanshker1@gmail.com

<sup>4</sup> Centre for Sustainable Energy Use in Food Chains, Institute of Energy Futures, Brunel University London, Kingston Lane, Uxbridge UB8 3PH, UK

<sup>5</sup> CanmetENERGY Research Centre, Natural Resources Canada, 1 Haanel Drive, Ottawa, ON K1A 1M1, Canada

\* Correspondence: pouyan.talebizadehsardari@brunel.ac.uk (P.T.); wahiba.yaici@canada.ca (W.Y.)



**Citation:** Lattieff, F.A.; Atiya, M.A.; Mahdi, J.M.; Majdi, H.S.; Talebizadehsardari, P.; Yaïci, W. Performance Analysis of a Solar Cooling System with Equal and Unequal Adsorption/Desorption Operating Time. *Energies* **2021**, *14*, 6749. <https://doi.org/10.3390/en14206749>

Academic Editor:  
Dimitrios Katsaprakakis

Received: 14 September 2021  
Accepted: 12 October 2021  
Published: 16 October 2021

**Publisher's Note:** MDPI stays neutral with regard to jurisdictional claims in published maps and institutional affiliations.



**Copyright:** © 2021 by the authors. Licensee MDPI, Basel, Switzerland. This article is an open access article distributed under the terms and conditions of the Creative Commons Attribution (CC BY) license (<https://creativecommons.org/licenses/by/4.0/>).

**Abstract:** In solar-thermal adsorption/desorption processes, it is not always possible to preserve equal operating times for the adsorption/desorption modes due to the fluctuating supply nature of the source which largely affects the system's operating conditions. This paper seeks to examine the impact of adopting unequal adsorption/desorption times on the entire cooling performance of solar adsorption systems. A cooling system with silica gel–water as adsorbent-adsorbate pair has been built and tested under the climatic condition of Iraq. A mathematical model has been established to predict the system performance, and the results are successfully validated via the experimental findings. The results show that, the system can be operational at the unequal adsorption/desorption times. The performance of the system with equal time is almost twice that of the unequal one. The roles of adsorption velocity, adsorption capacity, overall heat transfer coefficient, and the performance of the cooling system are also evaluated.

**Keywords:** solar energy; solar cooling; silica-gel-water; adsorption modeling

## 1. Introduction

Air conditioning (AC) is one of the primary human activities that contributes to heavy power consumption, particularly during the summer months. According to data provided by International Energy Agency (IEA, Paris, France), the global power consumed by air-conditioners and electric fans in building sector is around 20% of the total power consumption [1]. That, in turn, would exacerbate the environmental pollution since the key sources of electricity production worldwide are still fossil fuels (i.e., coal, oil, and natural gas). The traditional vapor-based compression cooling systems use ammonia [2], carbon dioxide [3], hydrofluorocarbons (HCFCs) [4], and recently hydrates [5,6] as refrigerants. These refrigerants, however, pose certain environmental risks. They can contribute to the global warming both directly via the release of refrigerant into the atmosphere and indirectly by the release of carbon oxides during the combustion of fossil fuels in the power plants that used to generate the electricity needed to keep the cooling equipment running. Solar adsorption cooling systems are found to be very efficient alternatives for dealing with these challenges. They neither use environment-damaging refrigerants, nor require fossil-fuel based electricity. These cooling systems can be driven by low grade energy like solar energy which is more abundant and more evenly distributed in nature than other energy sources. Moreover, the good solar radiation conditions in summer,

which closely corresponds to the periods when the peak demand for cooling is expected, enables the adsorption cooling to be a reliable technology for sustainable energy utilization. This technology can also aid to climate-change mitigation with making progress toward the United Nations sustainable development goals of reaching net-zero carbon emissions by the second half of the twenty-first century [7,8]. The main objective for utilizing the adsorption phenomenon in cooling systems is to improve the evaporation rate of the coolant fluid in use. This improves the system's cooling efficiency as the potential for removing more heat from the cooling space increases. Therefore, the cooling efficiency of adsorptive systems depends on the evaporation rate, which in turn, largely depends on the thermophysical properties of the adsorbent-adsorbate working pairs and the effective design of the porous adsorbent bed to provide the necessary heat and mass transfer augmentation. These influencing factors have been a subject of interest for numerous studies, and several cooling, refrigeration, and desalination applications have been explored using different working pairs with different bed designs [9–11]. The adsorption cycles with silica gel/water or zeolite/water as working pairs are found to be more functional than others for the use with solar panels or flat plate collectors as they can be powered by quite low, near ambient temperatures [12–14]. The two-chamber design for adsorption/desorption processes is usually applied to enable the adsorption chillers to operate alternatively so that intermittence-free cooling cycle is performed [15].

Many theoretical and technological advancements were conducted on water adsorbents like silica gel and zeolite to improve their utilization in the adsorption cooling systems. Miyazaki and Akisawa [16] examined the operating parameters of silica gel–water adsorption chiller based on single-bed design and observe that although increasing the size of adsorbent bed can decrease the coefficient of performance (COP) due to the shorter cycle time, it can also increase the specific cooling power (SCP). Wang et al. [17] measures how the pollution by the impurity ions or solid particles would increase the adsorption deterioration of silica gel, and found that soaking in acidic solution along with washing via distilled water would be a very good solution to restore the silica gel adsorption capacity. Effect of grain size and grain layers on the adsorption performance of silica gel was numerically examined by Chakraborty et al. [18]. It is found that COP and SCP can be both improved if smaller grain size is applied. Freni et al. [19] tested a novel composite of silica modified by calcium nitrate with water sorbent (SWS-8L) and the resulting COP based on experiments was 0.18–0.31 for cycle time of 10 min. Wang et al. [20] developed a lumped-parameter model for multi-bed silica adsorption chiller and showed that adopting a multi-bed design can enable the chiller to utilize heat source at a temperature as low as 65 °C more effectively than its mature two-bed technology. Manila et al. [21] proved through numerical simulation that the two-bed design with smaller cylinder's depth and optimum silica gel grain diameter of 0.8 mm is preferable for faster vapor uptake and lower bed pressure drop.

The good match between the high sunshine and the peak air-conditioning demand during summer represents the most feasible utilization of solar energy. Therefore, the feasibility of integrating solar collectors with adsorption chillers have been extensively investigated in literature. To enable more economic and technical feasibility of dual-stage absorption chillers in the building sector, Chemisana et al. [22] tested integrating of highly effective solar collectors (evacuated tube collectors) with adsorptive chillers to achieve driving temperatures as high as 150 °C and found that this arrangement can provide a substantial reduction in the collector area requirements. Habib et al. [23] evaluated by numerical simulation the single-stage and dual-stage operation modes of a four-bed silica gel-water adsorption chiller driven by evacuated tube collectors in Durgapur, India and found that the operation mode needs to be switched to dual-stage mode when the heat source temperature is below (60 °C). Drosou et al. [24] discussed the feasibility of parabolic trough collectors for use with solar adsorptive cooling system to cover the cooling needs of typical office building in Greece, and proved that the use of parabolic trough can bring higher COP within less space requirements compared to traditional flat plate collectors.

Wang et al. [25] studied the effect of the mass transfer on the performance of activated carbon-methanol adsorption chiller and demonstrated an improvement of 35.9% compared with the average COP of the natural mass transfer adsorption refrigeration system when the input radiation energy was not less than 14.7 MJ during a refrigeration cycle.

The performance of adsorption cooling systems powered by solar energy has been the subject of numerous research studies [26–32]. However, there were no reported studies adopting their performance under unequal adsorption/desorption phases times with long switching times. For an equal state, the time of adsorption is equal to the time of desorption. If there is a significant difference between the two phases (adsorption/desorption) times it is called unequal state. Under this circumstance of unequal state, the adsorption capacity rate is not equal to the desorption capacity rate. The difference of both states can lead to the distinct difference for the value of the system performance. However, in realistic cooling systems driven by solar energy, several factors have a strong effect on the adsorption/desorption phases times, especially for the systems that are operated under short cycle. For example, varying heating/cooling water temperatures or their mass flow rates, as a result of equipment obsolescence and weather changes, are commonly arising in the real cooling process. Based on these characteristics, this paper presents a dynamic model for an adsorption cooling system driven by solar evacuated tubes collectors under unequal states conditions. The existence of varying adsorption/desorption times with long switching times for a single bed cooling system was investigated experimentally in our earlier work [26]. Moreover, the minimum adsorption time for the present system is fixed, which indicates the shortest adsorption time at which the system still in service of producing cooling effect. Thus, the influence of the unequal state needs to be considered and cannot be neglected for obtaining the best model results. During these analyses, the roles of adsorption velocity, adsorption capacity, overall heat transfer coefficient, and the performance of the cooling system are also elucidated.

## 2. System Description

A schematic diagram of the main arrangements of the adsorption cooling system under investigation is illustrated in Figure 1. This system has been built and implemented by Lattief et al. [33] for solar-powered adsorption air-conditioning application under the climatic conditions of Iraq. In the present study, the same system has been retested under the unequal adsorption/desorption operating time conditions. The principal innovation of this concept is the capability to run the cooling system under different operation conditions with variable adsorption/desorption intervals. The system consists of three components, namely: the supplier of hot water which uses a set of solar evacuated-tube collectors as heat source, the supplier of cool water which is obtained from the municipality network, and the adsorption chiller equipment. The chiller which is considered the main component consists of four smaller parts: adsorber, evaporator, condenser, and set of valves that are operating on an intermittent basis according to whether the active mode is adsorption or desorption. The adsorber is fabricated as a shell-and-tube heat exchanger having diameters 17-mm ID and 19-mm OD with total heat-transfer area for the adsorber of 0.35 m<sup>2</sup>. The tube is made of copper embedded in silica-gel adsorbent type A as the shell of adsorber heat exchanger. The adsorbent was embedded in an aluminum mesh for enhancing the rates of heat and mass transfer inside the adsorber. The condenser is fabricated as 1-m coil tube inserted in a metal outer shell currying 2-L volumetric capacity of stagnant water. The evaporator is a small cylindrical vessel containing 0.25 L of distilled water as coolant located at the bottom of the chiller equipment.

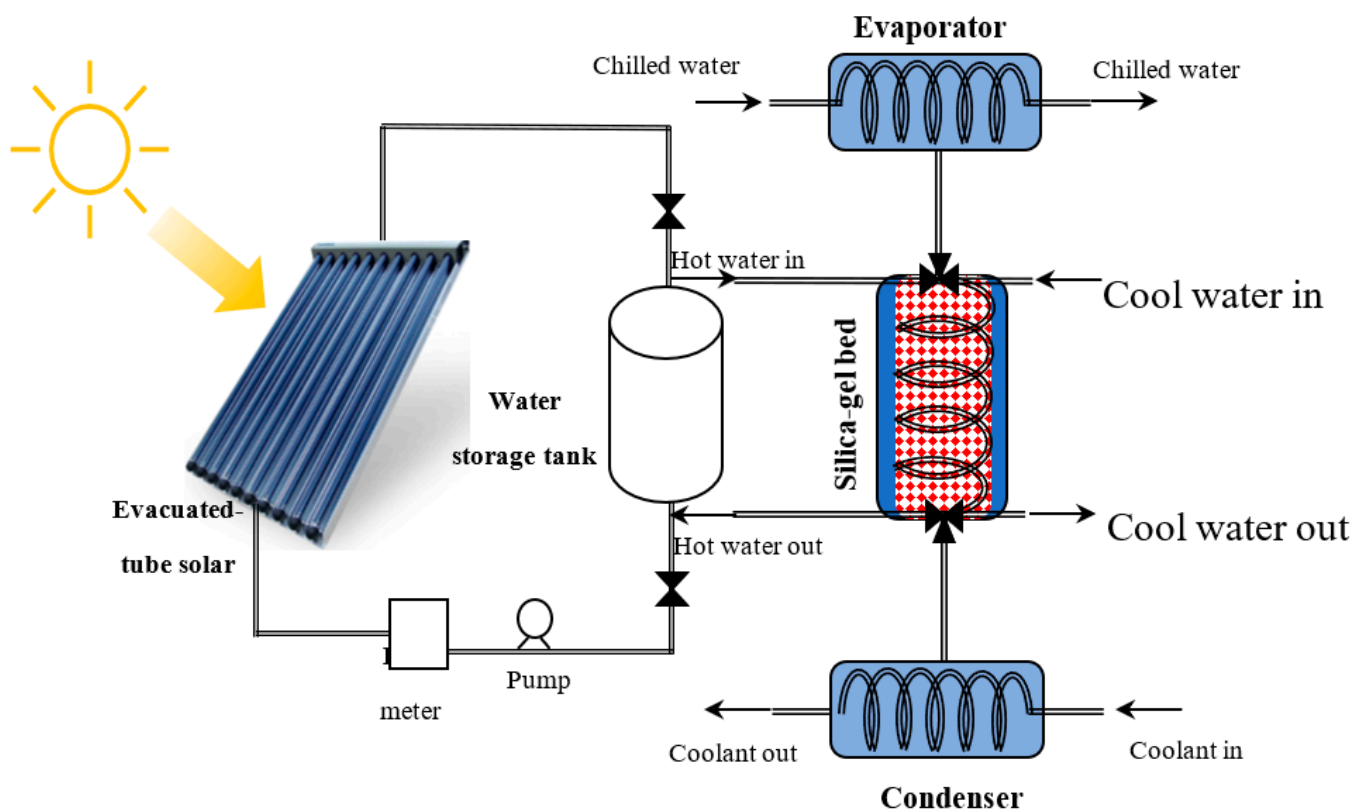


Figure 1. Schematic diagram of solar A/D cooling cycle.

A solar water heater consisting of two evacuated tube collectors, which were made up of parallel rows of transparent glass tubes and manufactured by gtc-solar co.ltd./China, was used to provide the required heating load. Each collector consists of a set of 20 evacuated tubes of 1.25 m in length and 0.025 m in diameter. A cylindrical storage tank with a capacity of 0.12 m<sup>3</sup> was used for collecting the hot water from the solar heater. A hydraulic pump was used to transport by forced circulation the heat-transfer fluid to the collectors. A rotameter (Model DH4500/LZS) with accuracy of  $\pm 4\%$  and measuring range of 20–170 L/min was used for water flow rate measurements. The scenario begins when the silica-gel bed is linked firstly to the evaporator for achieving the first half of the cycle, i.e., the adsorption mode. Once the evaporation comes to end up at the evaporator side, the silica gel in the bed side gets saturated with water vapor that is being drawn from the evaporator. Since adsorption is classified as an exothermic process, the existence of an external cooling is necessary for cooling the silica gel down so that a continuous uptake of vapor is preserved. In the second half of the cycle, the bed is linked to the condenser to condensate the water vapor by releasing its heat content to the coolant flowing in the condenser. In between these two processes, there is a process when water vapor circulation is stopped by closing all coolant valves. This process is known as the preheating/precooling process. The proposed operating time for each process in the cycle is: 10-min pre-heating, 20-min desorption, 20-min pre-cooling, and 10-min adsorption.

### 3. Mathematical Modelling

In order to evaluate the efficiency of the adsorption cooling system under the conditions of unequal adsorption/desorption times, a mathematical model of the adsorption/desorption (A/D) cycle was developed and validated. This model employs an interconnected cycle of the evaporator, condenser, and adsorber components to analyze the efficiency of the cooling system. The hot water flowrate is assumed to be constant during the desorption half cycle, and the cooling water flowrate undergoes a fluctuation during the next adsorption half cycle. In this model, the chiller system is assumed to be operating

with equal mode (10 min pre-heating + 20 min desorption + 10 min pre-cooling + 20 min adsorption) to demonstrate the effectiveness of unexpected physical changes on the system performance. In evaluating the model being developed, the mass and energy balances of silica gel-water as the adsorbent-adsorbed pair is used under the relevant temperature and pressure operating conditions. The lumped-parameter mathematical model of the adsorption chiller is employed to predict the temperature and coolant concentration variation in the bed. Then, the influence of shifting the cycle time from unequal mode to equal one on the performance of the chiller is discussed from the viewpoint of the COP and SCP.

The energy balances that govern the temperature distribution in the adsorber bed during the adsorption and desorption modes are expressed as

$$(M_s C p_s + M_s C p_{wr} x + M_{ml} C p_{ml}) \frac{dT_b}{dt} = m_{hw} C p_{hw} (T_{hwi} - T_{hwo}) + (\Delta H_a - C p_{wr} T_b) M_s \frac{dx_{des}}{dt} \quad (1)$$

$$(M_s C p_s + M_s C p_{wr} x + M_{ml} C p_{ml}) \frac{dT_b}{dt} = m_{cw} C p_{cw} (T_{cwi} - T_{cwo}) + (\Delta H_a - C p_{wr} T_b) M_s \frac{dx_{ads}}{dt} \quad (2)$$

where the left-hand side represents the change rate of sensible heat in the adsorber bed components, including the adsorbent material, adsorbate material and metal tubes. The right-hand side includes the rates of heat input and heat release during adsorption. The outlet temperature of the hot water ( $T_{hwo}$ ) from adsorption bed and cold water from desorper  $T_{cwo}$  are estimated using the log mean temperature difference (LMTD) method as

$$T_{hwo} = T_b + (T_{hwi} - T_b) \exp\left(-\frac{U_b A_b}{m_{hw} C p_{hw}}\right) \quad (3)$$

$$T_{cwo} = T_b + (T_{cwi} - T_b) \exp\left(-\frac{U_b A_b}{m_{cw} C p_{cw}}\right) \quad (4)$$

where  $\Delta H_a$ ,  $M_s C p_s$ ,  $M_s C p_{wr} x$ , and  $M_{ml} C p_{ml}$  represents the heat of adsorption, silica-gel heat capacity, heat capacity of adsorbed water, heat capacity of metallic part in the A/D bed, respectively.

In condenser, the energy balance is expressed as

$$\begin{aligned} & (M_c, wr C p_{wr} + M_{c,ml} C p_{c,ml}) \frac{dT_c}{dt} \\ & = m_{cw} C p_{cw} (T_{cwi} - T_{cwo}) - (\Delta H_e - C p_{wr} T_c) M_s \frac{dx_{des}}{dt} + C p_{wr} T_e M_s \frac{dx_{ads}}{dt} \end{aligned} \quad (5)$$

The outlet temperature of cooling water from the condenser is described by

$$T_{cwo} = T_c + (T_{cwi} - T_c) \exp\left(-\frac{U_c A_c}{m_{cw} C p_{cw}}\right) \quad (6)$$

In the evaporator, the energy balance is expressed as

$$(M_{e,wr} C p_{wr} + M_{e,ml} C p_{e,ml}) \frac{dT_e}{dt} = m_{ch} C p_{ch} (T_{chi} - T_{cho}) - (\Delta H_e - C p_{wr} (T_c - T_e)) M_s \frac{dx_{ads}}{dt} \quad (7)$$

The outlet temperature of chilled water from the evaporator is described by

$$T_{cho} = T_e + (T_{chi} - T_e) \exp\left(-\frac{U_e A_e}{m_{chw} C p_{chw}}\right) \quad (8)$$

The cooling effect in solar-powered A/D cycles is primarily attributed to how high is the uptake rate of the water vapor particles by the adsorbent materials. Therefore, the water adsorption/desorption rate ( $x$ ) is considered the major important parameter for evaluating the efficiency of adsorbent (silica-gel). The water adsorption/desorption rate is estimated using Dubinin-Astakhov model as

$$x^* = W_o \times \rho \times \exp\left[-k_m \times \left(R T_b \ln\left(\frac{P_b}{P_{c/e}}\right)\right)^n\right] \quad (9)$$

where  $P_b$  is the saturation pressure of water vapor in the adsorption bed. It is estimated using the correlation:

$$P_b = 133.31 \times \left(\exp\left(18.1 - \frac{3820}{T_b + 273 - 46.1}\right)\right) \quad (10)$$

$K_m$  is referred to as the overall mass transfer coefficient being defined as

$$k_m = \left( \frac{15 \times D_o}{R_p^2} \right) \exp\left( \frac{-E_a}{RT_b} \right) \quad (11)$$

Here  $D_o$ ,  $R_p$ ,  $E_a$ , and  $R$  denote the surface diffusion factor of the adsorbate in absorbent particles, the radius of absorbent particles, the surface diffusion activation energy, and the universal gas constant. For silica gel-water, these parameters take the following numerical values:  $2.54 \times 10^{-4} \text{ m}^2/\text{s}$ ,  $3.5 \times 10^{-4} \text{ m}$ ,  $4.20 \times 10^4 \text{ J/mol}$ , and  $8.314 \text{ J/mol.K}$ , respectively. The linear driving force (LDF) model is employed for the estimation of the water uptake velocity by the adsorbent particles as

$$\frac{dx}{dt} = k_m \cdot (x^* - x) \quad (12)$$

The heat brought from the heat source during desorption mode ( $Q_{in}$ ) is estimated as:

$$Q_{in} = \dot{m}_{hot} C_{p_{hot}} \int_0^{t_{cycle}} (T_{hot_{in}} - T_{hot_{out}}) dt \quad (13)$$

The heat released by working fluid in the evaporator section ( $Q_{evap}$ ) is estimated as:

$$Q_{evap} = \dot{m}_{chill} C_{p_{chill}} \int_0^{t_{cycle}} (T_{chill_{in}} - T_{chill_{out}}) dt \quad (14)$$

Finally, the coefficient of performance (COP) and the specific cooling power (SCP) for one cycle can be estimated as:

$$\text{COP} = \frac{Q_{evap}}{Q_{in}} \quad (15)$$

$$\text{SCP} = \frac{Q_{evap}}{M_s} \quad (16)$$

The parameters used in the simulation model with their numerical values are listed in Table 1.

**Table 1.** Values adopted in formulation of the mathematical model.

Symbol	Value	Unit
$M_s$	10	kg
$C_{p_{wr}}$	4188	J/kg.K
$C_{p_{hw}}$	4204	J/kg.K
$C_{p_{cw}}$	4183	J/kg.K
$C_{p_{ch}}$	4188	J/kg.K
$U_b$	400–1000	W/m <sup>2</sup> .K
$U_e$	4000	W/m <sup>2</sup> .K
$U_c$	4000	W/m <sup>2</sup> .K
$M_{ml} C_{p_{ml}}$	40,890	J/kg
$M_{c,ml} C_{p_{c,ml}}$	1993	J/kg
$M_{e,ml} C_{p_{e,ml}}$	977	J/kg
$A_b$	0.35	m <sup>2</sup>
$A_c$	0.1	m <sup>2</sup>
$A_e$	0.1	m <sup>2</sup>
$\Delta H_a$	2800	kJ/kg
$\Delta H_e$	2459	kJ/kg
$M_{c,wr}$	2	kg
$M_{e,wr}$	0.25	kg

#### 4. Results and Discussion

The performance of the intermittent cooling system with different adsorption/desorption operating times was investigated in terms of adsorption velocity, adsorption capacity, overall heat transfer coefficient, COP, and SCP. After validation of the model developed with the experimental findings, a parametric analysis of the system performance under both the equal and unequal phases times was conducted and reported. The obtained results were calculated by considering the inlet mass flow rate of 50 L/min with total cycle time of 60 min being divided into 30 min for adsorption and 30 min for desorption. The flow rate of 50 L/min was selected as this rate yields the largest bed

temperature lift which causes a highest cooling capacity. Increasing the cycle time more than 30 min has an insignificant effect on the cooling capacity. Therefore, adsorption/desorption time of 30 min was chosen to run this system. The performance of this proposed system in terms of (SCP and COP) was evaluated by using dynamic model to calculate the adsorption time variation that simulates the actual operation of the real system (single bed).

Figure 2 depicts the variation of the bed temperature with the cycle time for both cases, equal and unequal adsorption/desorption phases times. A coincide agreement can be observed in the first 30 min during desorption phase, while during the adsorption phase a slight deviation can be noticed at the last 10 min when the unequal adsorption phase is starting. This is because the unequal state has a long pre-cooling time (20 min) and the short adsorption time (10 min) that makes the adsorber pressure is much lower than the evaporator pressure. Moreover, starting the unequal adsorption process resulted in a larger amount of adsorbed water vapor and this is quite crucial to affect the bed temperature. Identical trend for both states confirm the validity of the model.

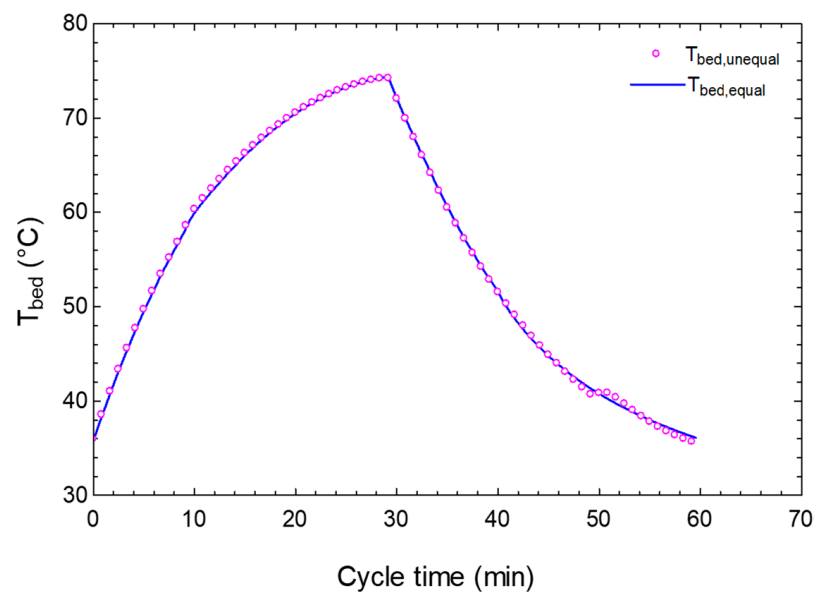


Figure 2. Bed temperature profile.

Figure 3 shows that the desorption velocity, 0.00012 kg water/kg silica.s, is highest at the start of the desorption process and becomes very slow after 20 min of operation. As per this figure, the adsorption velocity for both states rise sharply at the starting of the adsorption phase, but after that they move to decrease gradually with the progress of time. However, the unequal state has a maximum adsorption velocity value of about 0.0002 kg water/kg silica.s, which is noticeably higher than that of the equal state, 0.00008 kg water/kg silica.s. The reason of this difference is due to the variance in pressure between the evaporator and the adsorber as previously mentioned in Figure 2 and this difference is reduced to a very small value. It can be concluded that the faster the adsorption velocity is, the lower the cycle time becomes. The figure also indicates that the system can be driven more stably and efficiently by the equal state. This information is very useful when managing a cooling system being tailored to operate at the optimum adsorption velocity. This result is comparable to that founded by Yang PZ [34] who reported that the adsorption/desorption will not completely accomplish and the cooling potential of the adsorber cannot exert deeply if the adsorption time is too short.

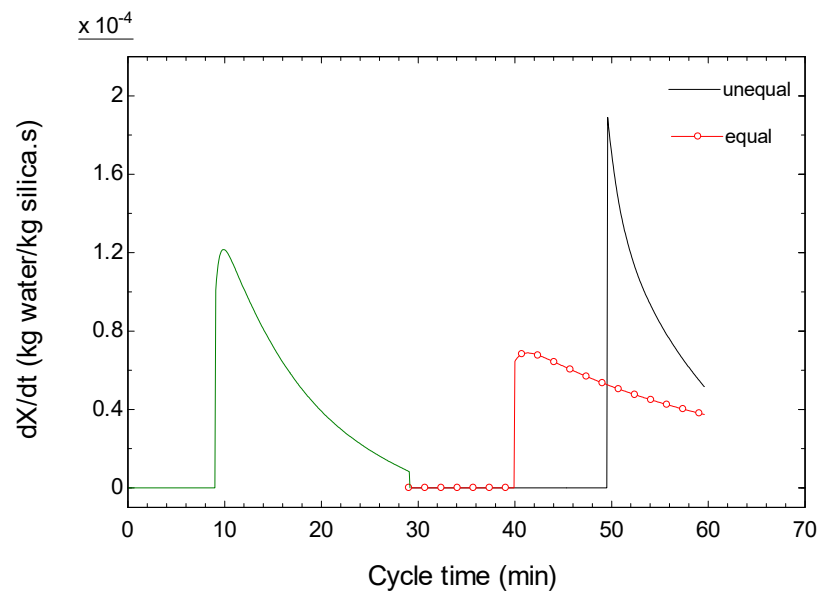


Figure 3. Adsorption velocity rate variation.

A complete cycle of adsorption/desorption for the silica gel-water adsorber is shown in Figure 4. As seen in this figure, desorption process is very close in concentration change to adsorption process, and many studies assume that both are the same in adsorption refrigeration process. During the desorption phase, the minimum value reached is 0.06 kg/kg after the first half-cycle of 30 min, and during the second half-cycle of 60 min, the maximum is 0.12 and 0.124 kg/kg for unequal and equal cycles, respectively. It is clear that changes in adsorption rate with time are not simultaneous. This means that the adsorption rate cannot be entirely reached when the unequal adsorption time reaches its end value. Using these results, it was determined that 4% of silica gel was not effectively used in unequal cycle compared with equal cycle. It could be observed that the equal adsorption rate deviates from the unequal one and this deviation does not seem very high at the adsorption completion point. Without doubt, the unequal state is influenced by the real process of cooling system and should not be neglected on designing cycle adsorption chiller, especially when the cycle is short because in real short cycle, the adsorbed water could not be sufficient due to the non-equilibrium adsorption process [35].

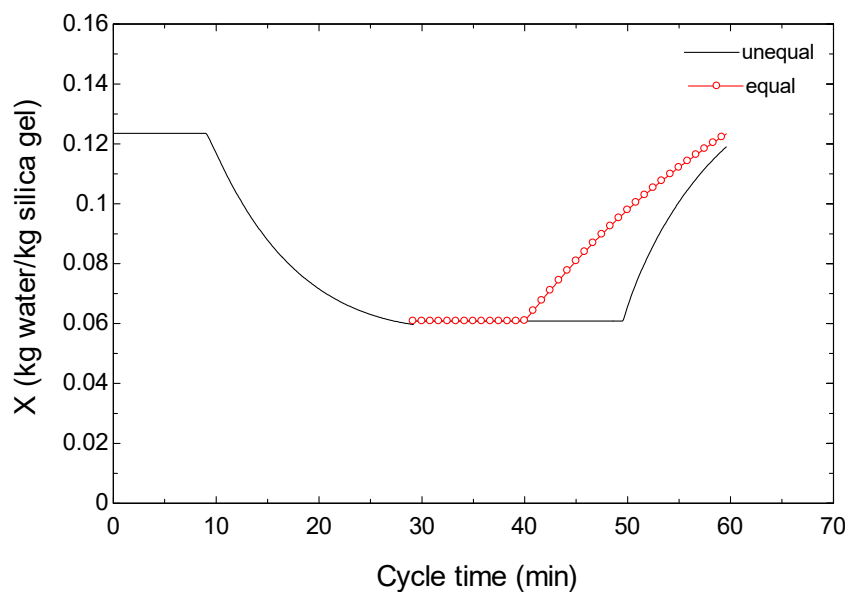


Figure 4. Adsorption capacity rate variation.



Figure 5 aims to determine the amount of exchanged water vapor involved in one adsorption/desorption cycle. It can be noticed that the bed is able to exchange a large amount of 0.064 kg/kg.s under equal condition and 0.06 kg/kg.s under unequal condition, so it is typical for air conditioning applications. The main reason for such differences between the equal and the unequal simulated data presented in Figure 5, would be the pre-assumption that the governing parameters like density, specific heat, and viscosity of the working fluid are pressure and temperature independent. Another reason would be the adoption of a simplified mathematical model for the heat-and-mass transfer simulation. It is worth to mention that the results of this work reveal low values compared with the other previous works [19,36,37].

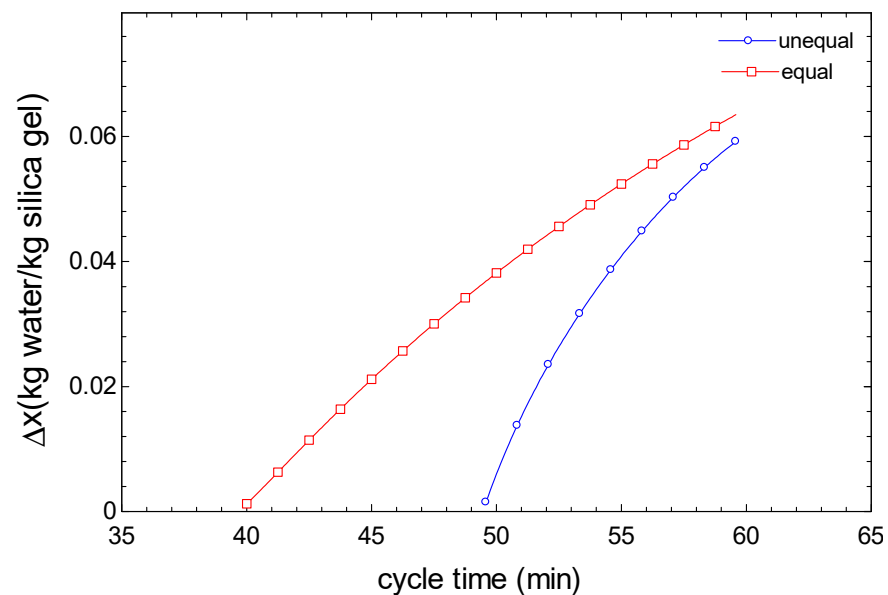


Figure 5. Adsorption/desorption exchange rates variance.

It can be realized that by far the heat-and-mass transfer problems in adsorptive cooling systems are not fully solvable. The major obstacle that prevents the employing of the adsorption cooling for widespread use is the low heat-and-mass transfer in the adsorption cooling system. Therefore, enhancing the heat-and-mass transfer in the adsorber to obtain faster adsorption/desorption rates is the key for boosting a superior adsorption cooling efficiency. In Figure 6, we have reported the overall heat transfer model results; the figure depicts the equal and unequal times evaluation of predicated overall heat transfer coefficient. The comparison between these values shows a significant difference. This difference may be due to the amount of the adsorbed water vapor is also not stable and is changing with time. Yet, the lack of an efficient thermal interaction between the adsorbent and the metal part of the adsorber results in an undesirable steep temperature gradient at the contact surface. As a matter of fact, stimulating the adsorbent to be in a good direct contact with the metal is not easy in practice, particularly when granular adsorbent is utilized. Therefore, several alternative designs of adsorptive cooling systems were proposed to mainly improve the internal heat and mass transfer [38–42]. In the majority of these systems, a constant  $U_b$  value is assumed for implementing their models, but they couldn't fully achieve the complete convergence. This work proves that the use of variable heat transfer coefficient gives more accurate and realistic results with closer convergence between the model results and the experimental data. It is clear that the heat transfer coefficient of the equal state is constant because of the semi-stable adsorption velocity as shown in Figure 3. Unequal heat transfer coefficient results show a similar trend to that of adsorption velocity trend depicted in Figure 3. It indicates the effect of the adsorption process on the heat transport rate between the adsorbent and its heat exchanger.

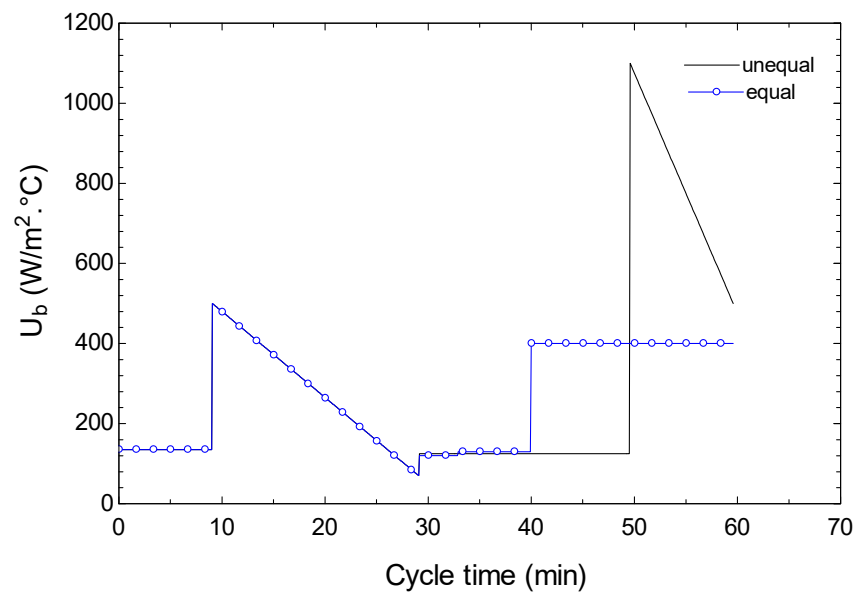


Figure 6. Overall heat transfer coefficient profile for the adsorber.

Variation of the desorbed water in the condenser with cycle time is predicted in Figure 7. It is clear that the condensate water rises sharply due the flow of the vapor from the desorber, then after it decreases due to the decrease in the amount of water vapor in the condenser. During adsorption phase, it can be seen that the condensate water is of about 0.6 kg for equal state and 0.57 kg for unequal state. There is a difference of 5% in condensate water between the two states. The results demonstrated that the condenser performance, for given operating conditions, is not strongly dependent on the adsorption steps.

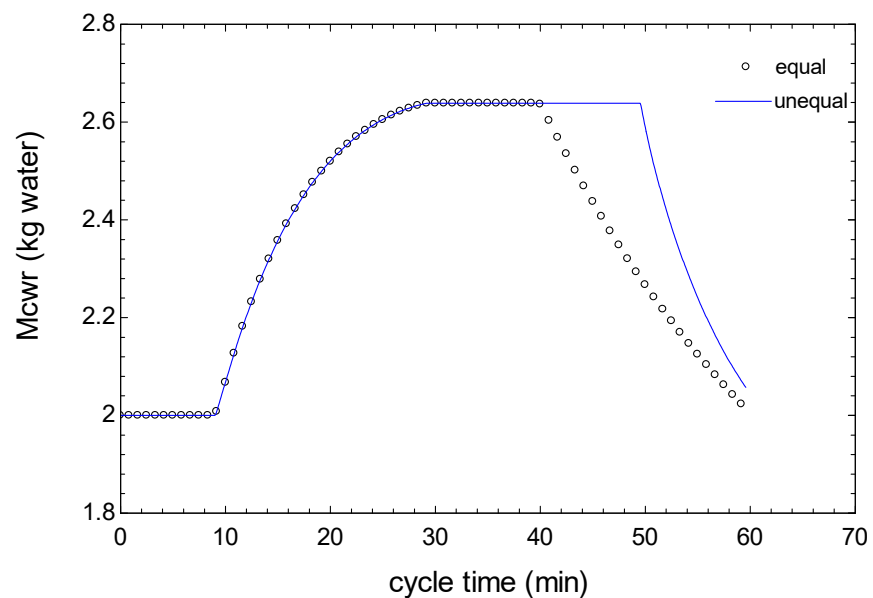


Figure 7. Condensate water profile in the condenser.

Figure 8 shows the variation of evaporating temperature with the cycle time. A good agreement can be observed between the unequal model results and the experimental data. Results of the equal model show a different behavior with a lower evaporating temperature. In comparison to the unequal cycle, the proposed equal cycle is capable of producing chilled water at a temperature below that of the unequal cycle, producing a cooling effect such as that achieved via the proposed equal cycle is almost impossible in practice. However, the proposed cycle mode enables generating a cooling effect and cold chilled water in either the adsorption or desorption mode. Thus,

in each mode of the cycle, there is at least one bed is linked to the evaporator so that the cooling effect can be interminably produced. Additionally, it can be seen that during a period of 40 min of equal state, the evaporating temperature increases from 9 to 12.2 °C and to 14 °C for unequal state when the pre-cooling phase extended to 50 min. This difference in temperature does not seem very big (1.6 °C) although there is a difference in time of adsorption, 10 min, between the two cycles. Furthermore, to keep the temperature of refrigerant inside the evaporator as low as possible, the evaporator was insulated tightly. Additionally, the results showed that equal adsorption capacity decreased the evaporator temperature to 6.6 °C, while the equal adsorption capacity resulted in a lower evaporator temperature of 5.8 °C. This indicates that the system is working with a good statement for both capacities and a high vacuum is generated due to the high performance of the adsorption process.

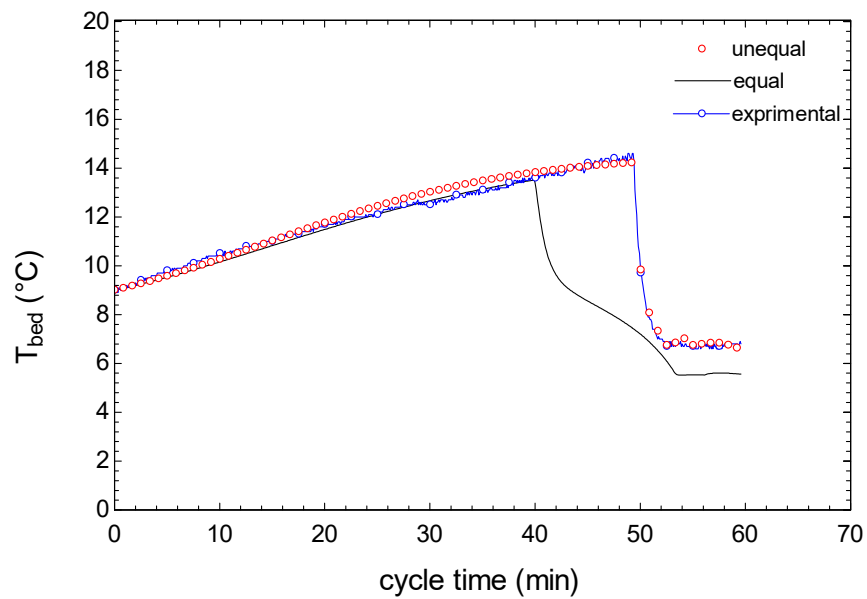
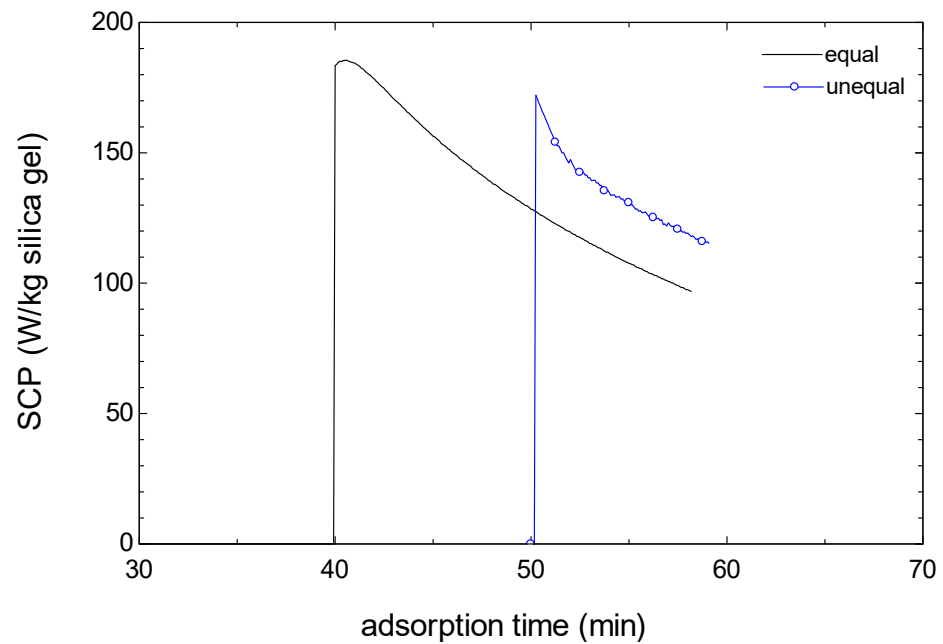


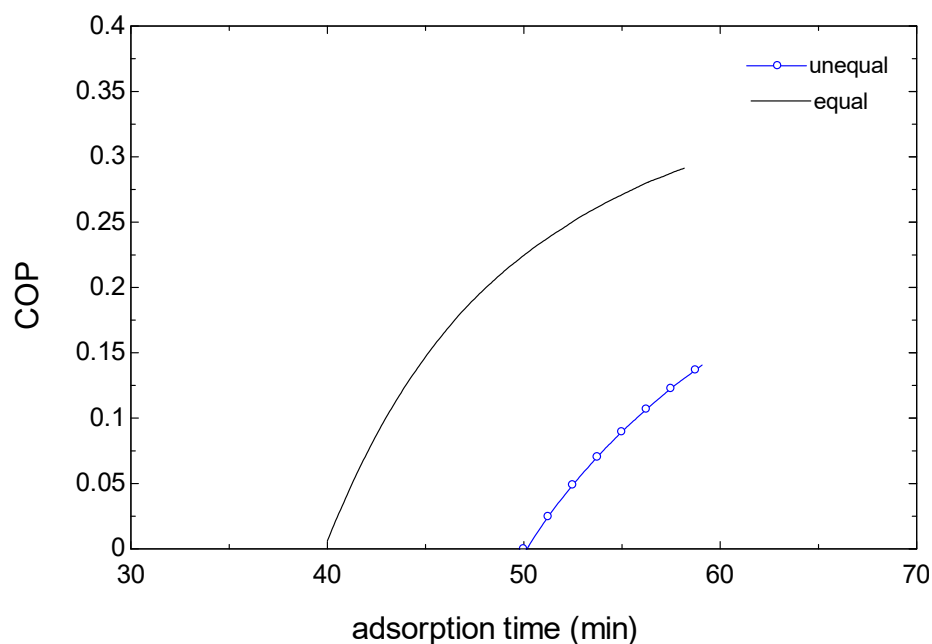
Figure 8. Temperature profile of the evaporator.

Figure 9 shows that the equal cycle produces a higher SCP as compared to that of the unequal cycle. According to this figure the SCP rises sharply at the beginning of the adsorption phase for both cycles. Afterward, this SCP decreases gradually with the progress in the adsorption process. The possible reason is that at the starting of adsorption, the silica gel has the lowest adsorption capacity, so water can be adsorbed by silica gel easily. As the process of adsorption goes, adsorption amount declines, and so does the production of the cooling effect. As seen in this figure, the SCP peak value of equal cycle is 185 W/kg, which is higher than that of unequal cycle, 120 W/kg, there is 35% an increment in SCP value for the equal cycle, although the adsorption velocity for the former cycle is lower than the latter cycle. In contrast, the adsorption capacity rate ( $x$ ) and the adsorption exchanged rate ( $\Delta x$ ) are higher for the equal cycle. It can be noted that the adsorption velocity has a lower effect on the SCP than the amount of the adsorbed refrigerant. However, increasing the SCP leads to increase the cooling effect inside the evaporator, and this increases the performance of the system. Without doubt, the unequal cycle model should be accounted and not be neglected on designing cycle adsorption cooling system, especially when the cycle is varied because in real system, the adsorbed refrigerant could not be sufficient due to the non-equilibrium adsorption process.



**Figure 9.** Specific cooling capacity variation.

Figure 10 has shown that the COP results of the equal adsorption process is similar in behavior to the unequal process and the reason is simply because of the high rate of the adsorption process. Those two figures give the dynamics of the system performance from the first time of adsorption phase up to the end of the phase. However, adsorption does not occur during the precooling phase while a decline in pressure exists, and the COP and SCP values are almost zero. Meanwhile, the COP value appears to almost increase linearly with the adsorption time as the cycle moves to the adsorption phase because the adsorption process is enhanced causing a higher cooling effect for a given heat input. The maximum COP value reached is 0.3 during the equal phase, and it is 0.15 during the unequal phase. Nonetheless, adequate performance can be achieved even for unequal cycle. In particular, the COP of 0.15 and SCP of 120 W/kg were estimated for the unequal cycle, demonstrating that it is still an acceptable value to work on and this system can be driven by a varied adsorption time. In general, there is a maximum of the COP at the equal cycle, but less adsorption velocity. Consequently, a strategy was adopted to assess the effect of the adsorption time. The different results are obtained for the COP and SCP: equaling the adsorption and desorption times leads to increase the system performance. For the two beds, equal time of adsorption and desorption phases is commonly used in cooling cycle but they are not always the same in the real system. A comparison with the results calculated by Angelo, et al. (2012) who employed similar conditions to those of our simulation ( $T_{des} = 90\text{ }^{\circ}\text{C}$ ,  $T_{cw} = 30\text{ }^{\circ}\text{C}$ ,  $T_e = 10\text{ }^{\circ}\text{C}$ ) shows that the peak value of the SCP is about 390 W/kg after 10 min, while for the present work, the peak value is 120 W/kg after 20 min. This difference in values is due to the different properties of the silica gel used in the two experiments. Angelo et al. used a “modified silica gel” which has an adsorption capacity rate exchange of  $\Delta x > 0.1\text{ kg water/kg silica gel}$ , whereas in our work a silica gel of  $\Delta x = 0.06\text{ kg water/kg silica gel}$  is used. Additionally, the maximum value of the COP (0.15) of our work is lower than that of Angelo’s experiment (0.41). The reason is that the larger amount of heat is required to raise the larger amount of silica gel for our experiment (10 kg).



**Figure 10.** Performance profile.

## 5. Conclusions

In this study, a preliminary attempt was made to evaluate the impact of adopting unequal adsorption/desorption times on the entire cooling performance of solar adsorption systems. The results obtained confirm that the variation of the precooling-adsorption time can potentially alert the system performance. The simulation results were obtained considering the overall heat transfer coefficient for the condenser, evaporator, and adsorbent beds all as varied values. This approach has not been tested before in the open literature. It facilitates a better prediction capability of the impact of any physical variation on the cooling performance of the adsorption system, especially the adsorption time. The results indicate that decreasing the adsorption time in comparison to the desorption time (unequal cycle) results in a reduction of the SCP and COP by 35 and 50%, respectively. This is because the greater amount of the cooling effect will not find a sufficient time required to produce it. Equal time mode raises the amount of adsorbed water vapor in the evaporator, and consequently the rate of adsorption increases, resulting in a higher cooling capacity and a higher COP. Eventually, the system's thermal performance is largely dependent on the balance in time between adsorption and desorption phases.

**Author Contributions:** Conceptualization, F.A.L. and M.A.A.; methodology, J.M.M.; software, F.A.L.; validation, H.S.M., M.A.A. and P.T.; formal analysis, J.M.M.; investigation, F.A.L.; resources, W.Y.; data curation, M.A.A.; writing—original draft preparation, F.A.L. and J.M.M.; writing—review and editing, M.A.A.; visualization, P.T.; supervision, F.A.L.; project administration, H.S.M.; funding acquisition, W.Y. All authors have read and agreed to the published version of the manuscript.

**Funding:** This research was funded by the Iraqi Ministry of Higher Education and Scientific Research/ the Research and Development Department/ the Program of Renewable and Sustainable Energy Projects, grant number 1613.

**Institutional Review Board Statement:** Not applicable.

**Informed Consent Statement:** Not applicable.

**Data Availability Statement:** Not applicable.

**Conflicts of Interest:** The authors declare no conflict of interest.

## Abbreviations

### Nomenclature

$A$	Heat exchange area ( $m^2$ )
$C_p$	Specific heat capacity ( $J/kg\ K$ )
$D_o$	Surface diffusion factor ( $m^2/s$ )
$E_a$	Activation energy for surface diffusion ( $kJ/mol$ )
$g$	Acceleration of gravity ( $m/s^2$ )
$h_{fg}$	Latent enthalpy of water ( $kJ/kg$ )
$k$	Thermal conductivity ( $W/m\ K$ )
$k_m$	Overall mass transfer coefficient ( $m/s$ )
$A$	Heat exchange area ( $m^2$ )
$C_p$	Specific heat capacity ( $J/kg\ K$ )
$D_o$	Surface diffusion factor ( $m^2/s$ )
$E_a$	Activation energy for surface diffusion ( $kJ/mol$ )
$g$	Acceleration of gravity ( $m/s^2$ )
$h_{fg}$	Latent enthalpy of water ( $kJ/kg$ )
$k$	Thermal conductivity ( $W/m\ K$ )
$k_m$	Overall mass transfer coefficient ( $m/s$ )
$M$	Mass ( $kg$ )
$P$	pressure ( $Pa$ )
$R$	Universal gas constant ( $kJ/kg\cdot K$ )
$R_p$	Average radius of absorbent particles ( $m$ )
$T$	Temperature ( $K$ )
$t$	Time ( $s$ )
$x$	water adsorption/desorption rate ( $x$ )
$U$	Overall heat transfer coefficient ( $W/m^2\cdot K$ )

### Abbreviation

A/D	Adsorption/desorption
D-A	Dubinin—Astakhov
COP	Coefficient of performance
LDF	Linear Driving Force
LMTD	Log mean temperature difference
SCP	Specific cooling power ( $W/kg$ )

### Subscripts

Ads	Adsorption
b	Adsorption/desorption bed
chill	Chilled water
c	Condenser
cw	Cold water
Des	Desorption
e	Evaporator
hw	Hot water
in	Inlet
s	Silica gel
wr	Water refrigerant
ml	Metal
out	Outlet
w	Water

## References

1. The Future of Cooling: Opportunities For Energy-Efficient Air Conditioning. Available online: <https://www.iea.org/> (accessed on 25 November 2019).
2. Tao, Y.; Hwang, Y.; Radermacher, R.; Wang, C. Experimental study on electrochemical compression of ammonia and carbon dioxide for vapor compression refrigeration system. *Int. J. Refrig.* **2019**, *104*, 180–188. [[CrossRef](#)]
3. Mohammadi, K.; Powell, K. Thermodynamic and economic analysis of different cogeneration and trigeneration systems based on carbon dioxide vapor compression refrigeration systems. *Appl. Therm. Eng.* **2020**, *164*, 114503. [[CrossRef](#)]

4. La Rocca, V.; Panno, G. Experimental performance evaluation of a vapour compression refrigerating plant when replacing R22 with alternative refrigerants. *Appl. Energy* **2011**, *88*, 2809–2815. [CrossRef]
5. Hassanpouryouzband, A.; Joonaki, E.; Farahani, M.V.; Takeya, S.; Ruppel, C.; Yang, J.; English, N.J.; Schicks, J.M.; Edlmann, K.; Mehrabian, H. Gas hydrates in sustainable chemistry. *Chem. Soc. Rev.* **2020**, *49*, 5225–5309. [CrossRef]
6. Matsuura, R.; Watanabe, K.; Yamauchi, Y.; Sato, H.; Chen, L.-J.; Ohmura, R. Thermodynamic analysis of hydrate-based refrigeration cycle. *Energy* **2021**, *220*, 119652. [CrossRef]
7. Masson-Delmotte, V.; Zhai, P.; Pörtner, H.-O.; Roberts, D.; Skea, J.; Shukla, P.R.; Pirani, A.; Moufouma-Okia, W.; Péan, C.; Pidcock, R. Global Warming of 1.5 C. 2018, 1. Available online: <https://apps.ipcc.ch/outreach/documents/451/1551801374.pdf> (accessed on 25 November 2019).
8. Hassanpouryouzband, A.; Joonaki, E.; Edlmann, K.; Haszeldine, R.S. Offshore Geological Storage of Hydrogen: Is This Our Best Option to Achieve Net-Zero? *ACS Energy Lett.* **2021**, *6*, 2181–2186. [CrossRef]
9. Alsaman, A.S.; Askalany, A.A.; Harby, K.; Ahmed, M.S. A state of the art of hybrid adsorption desalination–cooling systems. *Renew. Sustain. Energy Rev.* **2016**, *58*, 692–703. [CrossRef]
10. Goyal, P.; Baredar, P.; Mittal, A.; Siddiqui, A.R. Adsorption refrigeration technology—An overview of theory and its solar energy applications. *Renew. Sustain. Energy Rev.* **2016**, *53*, 1389–1410. [CrossRef]
11. Ruthven, D.M. *Principles of Adsorption and Adsorption Processes*; John Wiley & Sons: Hoboken, NJ, USA, 1984.
12. Askalany, A.A.; Salem, M.; Ismael, I.M.; Ali, A.H.H.; Morsy, M.G.; Saha, B.B. An overview on adsorption pairs for cooling. *Renew. Sustain. Energy Rev.* **2013**, *19*, 565–572. [CrossRef]
13. Sah, R.P.; Choudhury, B.; Das, R.K. A review on adsorption cooling systems with silica gel and carbon as adsorbents. *Renew. Sustain. Energy Rev.* **2015**, *45*, 123–134. [CrossRef]
14. Shmroukh, A.N.; Ali, A.H.H.; Ookawara, S. Adsorption working pairs for adsorption cooling chillers: A review based on adsorption capacity and environmental impact. *Renew. Sustain. Energy Rev.* **2015**, *50*, 445–456. [CrossRef]
15. Alahmer, A.; Ajib, S.; Wang, X. Comprehensive strategies for performance improvement of adsorption air conditioning systems: A review. *Renew. Sustain. Energy Rev.* **2019**, *99*, 138–158. [CrossRef]
16. Miyazaki, T.; Akisawa, A. The influence of heat exchanger parameters on the optimum cycle time of adsorption chillers. *Appl. Therm. Eng.* **2009**, *29*, 2708–2717. [CrossRef]
17. Wang, D.; Zhang, J.; Xia, Y.; Han, Y.; Wang, S. Investigation of adsorption performance deterioration in silica gel–water adsorption refrigeration. *Energy Convers. Manag.* **2012**, *58*, 157–162. [CrossRef]
18. Chakraborty, A.; Saha, B.B.; Aristov, Y.I. Dynamic behaviors of adsorption chiller: Effects of the silica gel grain size and layers. *Energy* **2014**, *78*, 304–312. [CrossRef]
19. Freni, A.; Sapienza, A.; Glaznev, I.S.; Aristov, Y.I.; Restuccia, G. Experimental testing of a lab-scale adsorption chiller using a novel selective water sorbent “silica modified by calcium nitrate”. *Int. J. Refrig.* **2012**, *35*, 518–524. [CrossRef]
20. Wang, X.; He, Z.; Chua, H.T. Performance simulation of multi-bed silica gel–water adsorption chillers. *Int. J. Refrig.* **2015**, *52*, 32–41. [CrossRef]
21. Manila, M.R.; Mitra, S.; Dutta, P. Studies on dynamics of two-stage air cooled water/silica gel adsorption system. *Appl. Therm. Eng.* **2020**, *178*, 115552. [CrossRef]
22. Chemisana, D.; López-Villada, J.; Coronas, A.; Rosell, J.I.; Lodi, C. Building integration of concentrating systems for solar cooling applications. *Appl. Therm. Eng.* **2013**, *50*, 1472–1479. [CrossRef]
23. Habib, K.; Choudhury, B.; Chatterjee, P.K.; Saha, B.B. Study on a solar heat driven dual-mode adsorption chiller. *Energy* **2013**, *63*, 133–141. [CrossRef]
24. Drosou, V.; Kosmopoulos, P.; Papadopoulos, A. Solar cooling system using concentrating collectors for office buildings: A case study for Greece. *Renew. Energy* **2016**, *97*, 697–708. [CrossRef]
25. Wang, Y.; Li, M.; Ji, X.; Yu, Q.; Li, G.; Ma, X. Experimental study of the effect of enhanced mass transfer on the performance improvement of a solar-driven adsorption refrigeration system. *Appl. Energy* **2018**, *224*, 417–425. [CrossRef]
26. Vasta, S.; Freni, A.; Sapienza, A.; Costa, F.; Restuccia, G. Development and lab-test of a mobile adsorption air-conditioner. *Int. J. Refrig.* **2012**, *35*, 701–708. [CrossRef]
27. Clausse, M.; Alam, K.C.A.; Meunier, F. Residential air conditioning and heating by means of enhanced solar collectors coupled to an adsorption system. *Sol. Energy* **2008**, *82*, 885–892. [CrossRef]
28. Wang, X.; Bierwirth, A.; Christ, A.; Whittaker, P.; Regenauer-Lieb, K.; Chua, H.T. Application of geothermal absorption air-conditioning system: A case study. *Appl. Therm. Eng.* **2013**, *50*, 71–80. [CrossRef]
29. Lu, Z.S.; Wang, R.Z. Experimental performance investigation of small solar air-conditioning systems with different kinds of collectors and chillers. *Sol. Energy* **2014**, *110*, 7–14. [CrossRef]
30. Desideri, U.; Proietti, S.; Sdringola, P. Solar-powered cooling systems: Technical and economic analysis on industrial refrigeration and air-conditioning applications. *Appl. Energy* **2009**, *86*, 1376–1386. [CrossRef]
31. Hadj Ammar, M.A.; Benhaoua, B.; Bouras, F. Thermodynamic analysis and performance of an adsorption refrigeration system driven by solar collector. *Appl. Therm. Eng.* **2017**, *112*, 1289–1296. [CrossRef]
32. Kalkan, N.; Young, E.A.; Celiktas, A. Solar thermal air conditioning technology reducing the footprint of solar thermal air conditioning. *Renew. Sustain. Energy Rev.* **2012**, *16*, 6352–6383. [CrossRef]

33. Lattieff, F.A.; Atiya, M.A.; Al-Hemiri, A.A. Test of solar adsorption air-conditioning powered by evacuated tube collectors under the climatic conditions of Iraq. *Renew. Energy* **2019**, *142*, 20–29. [[CrossRef](#)]
34. Yang, P.-z. Heat and mass transfer in adsorbent bed with consideration of non-equilibrium adsorption. *Appl. Therm. Eng.* **2009**, *29*, 3198–3203. [[CrossRef](#)]
35. Wang, W.; Wang, R. Investigation of non-equilibrium adsorption character in solid adsorption refrigeration cycle. *Heat Mass Transf.* **2005**, *41*, 680–684. [[CrossRef](#)]
36. Deshmukh, V.; Joshi, S. Review: Use of composite adsorption in adsorption refrigeration. *Int. J. Innov. Technol. Creat. Eng.* **2012**, *2*, 11–16.
37. Habib, K.; Saha, B.B.; Chakraborty, A.; Oh, S.T.; Koyama, S. Study on solar driven combined adsorption refrigeration cycles in tropical climate. *Appl. Therm. Eng.* **2013**, *50*, 1582–1589. [[CrossRef](#)]
38. Hassan, H.; Mohamad, A.; Bennacer, R. Simulation of an adsorption solar cooling system. *Energy* **2011**, *36*, 530–537. [[CrossRef](#)]
39. Laidi, M.; Hanini, S. Optimal solar COP prediction of a solar-assisted adsorption refrigeration system working with activated carbon/methanol as working pairs using direct and inverse artificial neural network. *Int. J. Refrig.* **2013**, *36*, 247–257. [[CrossRef](#)]
40. Lu, Z.; Wang, R.; Xia, Z. Experimental analysis of an adsorption air conditioning with micro-porous silica gel–water. *Appl. Therm. Eng.* **2013**, *50*, 1015–1020. [[CrossRef](#)]
41. Zhao, Y.; Hu, E.; Blazewicz, A. A non-uniform pressure and transient boundary condition based dynamic modeling of the adsorption process of an adsorption refrigeration tube. *Appl. Energy* **2012**, *90*, 280–287. [[CrossRef](#)]
42. Alelyani, S.M.; Bertrand, W.K.; Zhang, Z.; Phelan, P.E. Experimental study of an evacuated tube solar adsorption cooling module and its optimal adsorbent bed design. *Sol. Energy* **2020**, *211*, 183–191. [[CrossRef](#)]